Joint Blocklength and Location Optimization for URLLC-enabled UAV Relay Systems

Cunhua Pan, Hong Ren, Yansha Deng, Maged Elkashlan, and Arumugam Nallanathan, *Fellow, IEEE*

***Abstract*—This letter considers the unmanned aerial vehicle (UAV)-enabled relay system to deliver command information under ultra-reliable and low-latency communication (URLLC) requirements. We aim to jointly optimize the blocklength allocation and the UAV's location to minimize the decoding error probability subject to the latency requirement. The achievable data rate under finite blocklength regime is adopted. A novel perturbation-based iterative algorithm is proposed to solve this problem. Simulation results show that the proposed algorithm can achieve the same performance as the exhaustive search method, and significantly outperforms the existing algorithms.**

***Index Terms*—UAV, URLLC, Short-packet transmission, Relay.**

I. Introduction

UAV-assisted communication has attracted extensive attention due to its fast deployment and favorable channel gain [1]. UAVs can also serve as relays to provide wireless connectivity between two devices without direct communication links [1]–[5]. Joint relay trajectory and power allocation was studied in [2]. In [3], UAV node placement and communication resource allocation were jointly optimized. In [4], Zhang *et al.* studied the joint trajectory and power optimization to minimize the outage probability. In [5], the throughput maximization problem was studied for a two-user broadcast channel, which can be regarded as a decode-forward relay system where each hop has the same rate.

In 2017, URLLC has been regarded as one of three pillar applications that should be supported in the 5G communications [6]. Applications requiring URLLC services include factory automation, autonomous driving, remote surgery, etc. In URLLC, short packet transmission is normally selected to support the low-latency transmission [7]. In this case, the conventional Shannon's capacity based on the law of large numbers is no longer applicable. The achievable capacity under short packet regime was first derived in [8], which is a complicated function of the system parameters.

Recently, [9] and [10] considered the delay issues in UAV communications. Mean packet transmission delay minimization problem was studied in [9] with multi-layer UAVs, while minimum-rate ratio for each user was considered in [10] to flexibly adjust the percentage of its delay-constrained data traffic. However, the latency requirement was not considered in [9], [10], and the Shannon's capacity formula was adopted.

C. Pan, H. Ren, M. Elkashlan and A. Nallanathan are with School of Electronic Engineering and Computer Science, Queen Mary University of London, London, E1 4NS, U.K. (Email:h.ren, c.pan, maged.elkashlan, a.nallanathan@qmul.ac.uk). Y. Deng is with the Department of Informatics, Kings College London, London WC2R 2LS, U.K. (e-mail:yansha.deng@kcl.ac.uk). This work is supported by the U.K. Engineering and the Physical Sciences Research Council under Grant EP/N029666/1 and Grant EP/N029720/1.

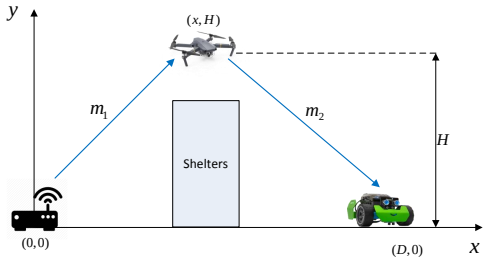

Fig. 1: UAV relay system for delivering URLLC services.

In this paper, we consider a downlink communication system in a frontline as shown in Fig. 1, where a central controller needs to send command information to a distant robot that performs certain reconnaissance missions in a military area. For concealment, shelters with thick cement/metal walls are built between the outside controller and the military area. Hence, the channel gain between the controller and the robot is weak and negligible, and requires a UAV to fly above the shelter to assist the transmission between the controller and the robot. We aim for jointly optimizing the location of the UAV and blocklength allocation of the UAV and the controller to minimize the decoding error probability subject to the latency and location constraints. To solve this problem, we propose a novel perturbation-based iterative algorithm to alternatively optimize the location and the blocklength. Our results show that the proposed low-complexity algorithm achieves almost the same performance as the exhaustive search method, and performs much better than the existing algorithms.

II. System Model

As shown in Fig. 1, we consider a two-dimensional UAV-enabled military surveillance scenario[1], where the UAV hovers at (x, H) above the horizontal line between the controller and the robot, with H as the fixed altitude. The locations of controller and robot are $(0, 0)$ and $(D, 0)$. The packet size of the command signal is L bits, whose transmission needs to be completed within $T_{\max}$ seconds. Then, the overall blocklength is $M = BT_{\max}$ [7], where B is the system bandwidth. Each transmission period has two phases, i.e., the first phase corresponds to the transmission from controller to UAV, while the second is from UAV to robot. The blocklength allocated for each phase is given by m_1 and m_2, respectively. The transmission powers from controller and UAV are fixed as P_1 and P_2, respectively.

[1]In this paper, we consider only one UAV and one robot since it may be easily discovered by the enemies with more UAVs and robots. In addition, the expression of the decoding error probability for multiple UAVs and robots is very complicated and difficult to optimize, which will be left for future work.

The channel power gain from the controller to the UAV, and that from the UAV to the robot are denoted as h_1 and h_2, respectively. According to the measurement result in [11], the LOS probability is close to one when the UAV is above a certain altitude (e.g. 120 m), and the free space channel model can be adopted. Thus, h_1 and h_2 can be represented as

$$h_1 = \frac{\beta_0}{H^2 + x^2}, h_2 = \frac{\beta_0}{H^2 + (D-x)^2}, \tag{1}$$

where β_0 is channel power gain at a reference distance of $d_0 = 1$ meter.

According to [8], to transmit a short packet of size L within m_1 symbols, the decoding error at the UAV is given by $\varepsilon_1 = Q\left(f\left(\gamma_1, m_1, L\right)\right)$, where $f\left(\gamma_1, m_1, L\right) = \ln 2\sqrt{\frac{m_1}{V_1}}\left(\log_2(1+\gamma_1) - \frac{L}{m_1}\right)$ with $\gamma_1 = P_1 h_1$ [2] and $V_1 = 1-(1+\gamma_1)^{-2}$. Similarly, the decoding error probability at the robot is given by $\varepsilon_2 = Q\left(f\left(\gamma_2, m_2, L\right)\right)$, where $\gamma_2 = P_2 h_2$.

We consider that the UAV acts as a decode-and-forward (DF) relay. Then, the overall decoding error probability from the controller to the robot is given by

$$\varepsilon = \varepsilon_1 + (1-\varepsilon_1)\varepsilon_2. \tag{2}$$

To enable URLLC, we aim to jointly optimize the location of the UAV and the blocklength for two phases to minimize the overall decoding error probability under the latency/blocklength constraint. Thus, the optimization problem can be formulated as

$$\min_{\{m_1, m_2, x\}} \quad \varepsilon \tag{3a}$$

$$\text{s.t.} \quad d_1 \le x \le d_2, \tag{3b}$$

$$m_1 + m_2 = M, \tag{3c}$$

$$m_1, m_2 \in \mathbb{Z}, \tag{3d}$$

where (3b) specifies the feasible region for x that mainly depends on the shape of the shelters, $\mathbb{Z}$ is the positive integer set. Problem (3) is difficult to solve due to: 1) the objective function is not jointly convex w.r.t. the optimization variables; 2) even with fixed blocklength or location, the objective function is not convex w.r.t. the location or the blocklength.

III. Low-complexity Algorithm

In this section, we develop a low-complexity iterative algorithm to solve Problem (3).

A. Optimize Blocklength Allocation with Fixed x

With fixed UAV location x, the channel gains h_1 and h_2 are fixed according to (1). Then, we only need to optimize the blocklength. Remind that the expression of objective function in (2) is very complicated. To handle this difficulty, we note that to guarantee the extremely low error probability for the whole link, the error probability for each link should be sufficiently small. In this case, we can approximate the overall error probability as $\varepsilon(m_1) \approx \varepsilon_1(m_1) + \varepsilon_2(m_1) \triangleq \tilde{\varepsilon}(m_1)$. In the following theorem, we prove that $\tilde{\varepsilon}(m_1)$ is a convex function of m_1.

Theorem 1: We assume that m_1 is a continuous variable. Given the channel gains h_1 and h_2, $\tilde{\varepsilon}(m_1)$ is a convex function w.r.t. m_1.

[2]The noise is normalized to unit.

Proof: We first prove that $\varepsilon_1(m_1)$ is a convex function w.r.t. m_1, then the convexity of function $\varepsilon_2(m_1)$ can be proved in a similar method by replacing m_2 with $M - m_1$. Thus, the summation of two convex functions $\tilde{\varepsilon}(m_1)$ is a convex function.

To simplify the notation, we denote $f_1(m_1) = f\left(\gamma_1, m_1, L\right)$. The first order and second order of $\varepsilon_1(m_1)$ w.r.t. m_1 are given by

$$\varepsilon_1'(m_1) = -\frac{1}{\sqrt{2\pi}} e^{-\frac{f_1^2(m_1)}{2}} f_1'(m_1), \tag{4}$$

$$\varepsilon_1''(m_1) = \frac{1}{\sqrt{2\pi}} e^{-\frac{f_1^2(m_1)}{2}} \left(f_1(m_1)(f_1'(m_1))^2 - f_1''(m_1)\right). \tag{5}$$

Since the first term in the brackets of (5) is positive, we only need to prove $f_1''(m_1) \le 0$ so that $\varepsilon_1(m_1)$ is a convex function.

To this end, we first simplify the function f_1 as

$$f_1(m_1) = A_1\sqrt{m_1}\left(C_1 - \frac{L}{m_1}\right), \tag{6}$$

where A_1 and C_1 are constants given by $A_1 = \ln 2/\sqrt{V_1}$ and $C_1 = \log_2(1+\gamma_1)$, respectively.

The first and second derivative of $f_1(m_1)$ w.r.t. m_1 are

$$f_1'(m_1) = \frac{1}{2}A_1 C_1 m_1^{-\frac{1}{2}} + \frac{1}{2}A_1 L m_1^{-\frac{3}{2}}, \tag{7}$$

$$f_1''(m_1) = -\frac{1}{4}A_1 C_1 m_1^{-\frac{3}{2}} - \frac{3}{4}A_1 L m_1^{-\frac{5}{2}} < 0, \tag{8}$$

which show that $f_1(m_1)$ is a strictly concave function of m_1. Then $\varepsilon_1(m_1)$ is a convex function w.r.t. m_1. By using the similar derivations, we show that $\varepsilon_2(m_1)$ is also a convex function w.r.t. m_1. This completes the proof. ■

Based on Theorem 1, we apply the bisection search method to find the optimal blocklength allocation through solving the following equation:

$$\tilde{\varepsilon}'(m_1) = \varepsilon_1'(m_1) + \varepsilon_2'(m_1) = 0. \tag{9}$$

The details are provided in Algorithm 1.

Algorithm 1: Find the Optimal m_1 and m_2 with Fixed x

Initialize $m_1^{\text{lb}} = 1, m_1^{\text{ub}} = M-1$ and the error tolerance $\delta = 0.5$;
while $m_1^{\text{ub}} - m_1^{\text{lb}} > \delta$ **do**
  Set $m_1^{\text{mid}} = (m_1^{\text{lb}} + m_1^{\text{ub}})/2$.
  if $\tilde{\varepsilon}'(m_1)|_{m_1 = m_1^{\text{mid}}} > 0$ **then**
    Set $m_1^{\text{ub}} = m_1^{\text{mid}}$.
  else
    Set $m_1^{\text{lb}} = m_1^{\text{mid}}$.
  end
end
Return the optimal m_1 as $m_1^* = \underset{\{\lfloor m_1^{\text{mid}} \rfloor, \lceil m_1^{\text{mid}} \rceil\}}{\arg\min} \tilde{\varepsilon}$ and the optimal m_2 as $m_2^* = M - m_1^*$.

B. Optimal Location Optimization with Fixed m_1 and m_2

In this subsection, we aim for optimizing location x with given m_1 and m_2. However, the objective function $\tilde{\varepsilon}(x)$ is not a convex function w.r.t. x. In the following, we numerically show that $\tilde{\varepsilon}(x)$ has only one local minimum point. Hence, there only exists only one solution that minimizes $\tilde{\varepsilon}(x)$.

To provide clear explanations, we define a new function $g(x) \triangleq \ln(\tilde{\varepsilon}(x))$, which has the same monotonic property of

$\tilde{\varepsilon}(x)$. We first obtain the first and second derivative of $g(x)$ w.r.t. x as follows. We define $f_1(x) = f(\gamma_1(x), m_1, L)$ and $f_2(x) = f(\gamma_2(x), m_2, L)$, where $\gamma_1(x)$ and $\gamma_2(x)$ are given by $\gamma_1(x) = \frac{P_1\beta_0}{H^2+x^2}$ and $\gamma_2(x) = \frac{P_2\beta_0}{H^2+(D-x)^2}$, respectively.

The first derivative of $g(x)$ w.r.t. x is given by

$$g'(x) = \frac{\varepsilon_1'(x) + \varepsilon_2'(x)}{\varepsilon_1(x) + \varepsilon_2(x)}, \tag{10}$$

where $\varepsilon_i'(x)$ is given by

$$\varepsilon_i'(x) = \frac{\partial \varepsilon_i(\gamma_i)}{\partial \gamma_i}\gamma_i'(x), i = 1, 2, \tag{11}$$

with $\gamma_i'(x)$ given by

$$\gamma_1'(x) = -\frac{2P_1\beta_0 x}{\left(H^2+x^2\right)^2}, \gamma_2'(x) = \frac{2P_2\beta_0(D-x)}{\left(H^2+(D-x)^2\right)^2}, \tag{12}$$

and $\frac{\partial \varepsilon_i(\gamma_i)}{\partial \gamma_i}$ given by

$$\frac{\partial \varepsilon_i(\gamma_i)}{\partial \gamma_i} = -\frac{1}{\sqrt{2\pi}} e^{-\frac{f_i^2(\gamma_i)}{2}} \frac{\partial f_i(\gamma_i)}{\partial \gamma_i}. \tag{13}$$

In (13), $\frac{\partial f_i(\gamma_i)}{\partial \gamma_i}$ is

$$\frac{\partial f_i(\gamma_i)}{\partial \gamma_i} = \sqrt{m_i} \frac{1 - \ln 2 \frac{\log_2(1+\gamma_i) - \frac{L}{m_i}}{(1+\gamma_i)^2 - 1}}{\sqrt{(1+\gamma_i)^2 - 1}}. \tag{14}$$

The second derivative of $g(x)$ w.r.t. x can be calculated as

$$g''(x) = \frac{\left(\varepsilon_1''(x) + \varepsilon_2''(x)\right)\left(\varepsilon_1(x) + \varepsilon_2(x)\right) - \left(\varepsilon_1'(x) + \varepsilon_2'(x)\right)^2}{\left(\varepsilon_1(x) + \varepsilon_2(x)\right)^2},$$

where $\varepsilon_i''(x), i = 1, 2$ are given by

$$\varepsilon_i''(x) = \frac{\partial^2 \varepsilon_i(\gamma_i)}{\partial \gamma_i^2}\left(\gamma_i'(x)\right)^2 + \frac{\partial \varepsilon_i(\gamma_i)}{\partial \gamma_i}\gamma_i''(x), \tag{15}$$

with $\gamma_i''(x)$ given by

$$\gamma_1''(x) = \frac{6P_1\beta_0 x^4 + 4P_1\beta_0 H^2 x^2 - 2P_1\beta_0 H^4}{\left(H^2+x^2\right)^4},$$

$$\gamma_2''(x) = \frac{6P_2\beta_0(D-x)^4 + 4P_2\beta_0 H^2(D-x)^2 - 2P_2\beta_0 H^4}{\left(H^2+(D-x)^2\right)^4},$$

and $\frac{\partial^2 \varepsilon_i(\gamma_i)}{\partial \gamma_i^2}$ given by

$$\frac{\partial^2 \varepsilon_i(\gamma_i)}{\partial \gamma_i^2} = \frac{1}{\sqrt{2\pi}} e^{-\frac{f_i^2(\gamma_i)}{2}} \left(f_i(\gamma_i) \left(\frac{\partial f_i(\gamma_i)}{\partial \gamma_i} \right)^2 - \frac{\partial^2 f_i(\gamma_i)}{\partial \gamma_i^2} \right). \tag{16}$$

In (16), $\frac{\partial^2 f_i(\gamma_i)}{\partial \gamma_i^2}$ is given by

$$\frac{\partial^2 f_i(\gamma_i)}{\partial \gamma_i^2} = c_i \left(-\frac{1}{1+\gamma_i} - (1+\gamma_i) \right) \left((1+\gamma_i)^2 - 1 \right) + 3c_i(1+\gamma_i) \left(\log_2(1+\gamma_i) - \frac{L}{m_i} \right) \ln 2, \tag{17}$$

where $c_i = \sqrt{m_i} \Big/ \left((1+\gamma_i)^2 - 1 \right)^{5/2}$.

Unfortunately, $g(x)$ is not a convex function w.r.t. x in the whole region of x. Fig. 2 plots the functions $g(x)$, $g'(x)$ and $g''(x)$ versus x. It is observed from this figure that when $0\text{m} < \text{x} < 142.5\text{m}$, $g''(x) < 0$, which means $g(x)$ is a concave function. On the other hand, when $142.5\text{m} < \text{x} < 186.5\text{m}$, $g''(x) > 0$ and $g(x)$ is a convex function. Finally, when $186.5\text{m} < \text{x} < 200\text{m}$, $g(x)$ becomes a concave function again. However, it is observed that $g'(x) > 0$ when $0\text{m} < \text{x} < 163.4\text{m}$, and $g'(x) < 0$ when $163.4\text{m} < \text{x} < 200\text{m}$. This means function $g(x)$ first decreases with x for $0\text{m} < \text{x} < 163.4\text{m}$ and then increases with x for $163.4\text{m} < \text{x} < 200\text{m}$, and there exists only one minimum value. It is difficult to rigorously prove this due to the cumbersome expression of $g'(x)$. We check all the other simulation parameters, all numerical results show the same trend of function $g(x)$ [3]. As a result, the bisection search can be used to find the root of $g'(x)$, details of which can be found in the following algorithm.

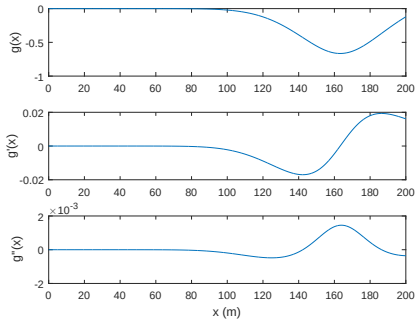

Fig. 2: $g(x)$, $g'(x)$ and $g''(x)$ versus x, where the system parameters are the same as those in the simulation section.

Algorithm 2: Find the Optimal x with Fixed m_1 and m_2

1 **Initialize** $x^{\text{lb}} = d_1, x^{\text{ub}} = d_2$ and error tolerance $\zeta = 0.1$;
2 **if** $g'(x)|_{x=d_2} < 0$ **then**
3 Return the optimal $x^* = d_2$.
4 **else**
5 **if** $g'(x)|_{x=d_1} > 0$ **then**
6 Return the optimal $x^* = d_1$.
7 **else**
8 **while** $x^{\text{ub}} - x^{\text{lb}} > \zeta$ **do**
9 Set $x^{\text{mid}} = (x^{\text{ub}} + x^{\text{lb}})/2$.
10 **if** $g'(x)|_{x=x^{\text{mid}}} > 0$ **then**
11 Set $x^{\text{up}} = x^{\text{mid}}$.
12 **else**
13 Set $x^{\text{lb}} = x^{\text{mid}}$.
14 **end**
15 **end**
16 **end**
17 **end**

C. Overall Algorithm and Analysis

It is noted from simulations that the conventional block coordinate descent method, which directly iterates between blocklength and location, is very likely to get stuck at the initial point. To overcome this issue, we introduce a small perturbation for the blocklength m_1 in each iteration as shown in line 4 of Algorithm 3, where $N_{\max}$ is a small integer.

The overall algorithm for solving Problem (3) is provided in Algorithm 3. The convergence of this algorithm is guaranteed since the objective value decreases in each step and the value is lower-bounded by zero. The complexity of this algorithm

[3]The rational behind this is that when x is small, the link from UAV to the robot will be the bottleneck of the whole link, and vice versa.

Algorithm 3: Iterative Algorithm for Solving Problem (3)

Initialize $m_1^{(0)}, m_2^{(0)}$ and $x^{(0)}$, integer parameter $N_{\max}$, iterative index $t = 1$, maximum iterative times $t_{\max}$;
repeat
  With given $x^{(t-1)}$, obtain the optimal $m_1^{(t)}$ by using Algorithm 1;
  Generate two random integer values n^l and n^r within $[1, N_{\max}]$. Use Algorithm 2 to calculate the optimal location when $m_1 = m_1^{(t)} - n^l, m_1^{(t)}, m_1^{(t)} + n^r$. The corresponding optimal x is denoted as $\mathcal{X}^{(t)} = \{x_l^{(t)}, x_m^{(t)}, x_r^{(t)}\}$. Choose the optimal x from $\mathcal{X}^{(t)}$ with the minimum $\tilde{\varepsilon}$, and denote it as $x^{(t)}$.
  Set $t = t + 1$;
until $t \geq t_{\max}$;

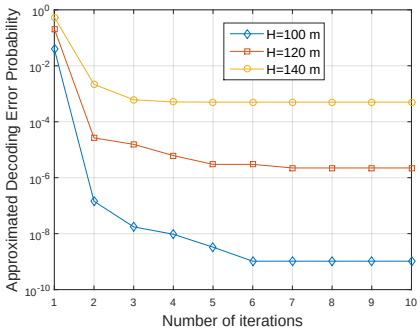

Fig. 3: Convergence behaviour of Algorithm 3 for various H.

is analyzed as follows. In each iteration of Algorithm 3, we need to run both Algorithm 1 only once and Algorithm 2 for three times. The complexity of Algorithm 1 is given by $Q_1 = \mathcal{O}(\log_2(M/\delta))$, while that of Algorithm 2 is $Q_2 = \mathcal{O}(\log_2((d_2 - d_1)/\zeta))$. Hence, the overall complexity of Algorithm 3 is given by $\mathcal{O}(n_{\max}(Q_1 + Q_2))$. In simulations, the algorithm generally converges within ten iterations.

By using the similar analysis, the complexity of exhaustive search method is given by $\mathcal{O}(M(d_2 - d_1)/\zeta)$, which is significantly higher that of Algorithm 3.

Although Algorithm 3 cannot be guaranteed to yield a globally optimal solution, simulations show this algorithm can achieve the same performance as the exhaustive method.

IV. Simulation Results

We now perform simulation results to show the performance of our proposed algorithm. The system parameters are set as follows: system bandwidth of $B = 1$ MHz, $D = 200$ m, $H = 120$ m, $d_1 = 30$ m, $d_2 = 130$ m, $L = 100$ bits, $M = 100$, $\beta_0 = 50$ dB, $P_1 = 3$ Watt, $P_2 = 1$ Watt, $N_{\max} = 3$, $t_{\max} = 10$. The system transmission delay duration is set as $T_{\max} = 100$ us. Thus, the total number of symbols is $M = BT_{\max} = 100$.

In Fig. 3, we plot the convergence behaviour of Algorithm 3 for various H. It is shown in Fig. 3 that the algorithm converges rapidly and generally ten iterations are enough for convergence for all considered H, which indicates that our algorithm has a low complexity.

In Fig. 4, we compared the proposed algorithm with the following algorithms: 1) exhaustive search algorithm (labeled as 'Exhaus.'), 2) optimal blocklength allocation with fixed location $x = (d_1 + d_2)/2$ (labeled as 'Fixedx'), and 3) the optimal location with fixed blocklength $m_1 = M/2$ (labeled as 'Fixedm'). It is seen from Fig. 4 that the proposed algorithm achieves the same performance as that of the exhaustive search algorithm, and significantly outperforms the other two algorithms, which emphasizes the importance of joint optimization.

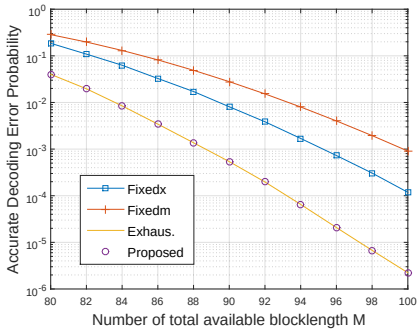

Fig. 4: Performance comparison for various algorithms.

V. Conclusions

This paper studied the joint location and blocklength allocation for UAV relay system with URLLC requirement. An effective low-complexity iterative algorithm was proposed to solve the optimization problem. Each subproblem can be solved by using the bisection search method. Simulation results confirm that the proposed algorithm achieved the same performance as that of the exhaustive search method, and has superior performance over the existing algorithms.

References

[1] Y. Zeng, R. Zhang, and T. J. Lim, "Wireless communications with unmanned aerial vehicles: opportunities and challenges," *IEEE Commun. Mag.*,, vol. 54, no. 5, pp. 36–42, May 2016.

[2] ——, "Throughput maximization for UAV-enabled mobile relaying systems," *IEEE Trans. Commun.*, vol. 64, no. 12, pp. 4983–4996, Dec 2016.

[3] R. Fan, J. Cui, S. Jin *et al.*, "Optimal node placement and resource allocation for UAV relaying network," *IEEE Commun. Lett.*, vol. 22, no. 4, pp. 808–811, April 2018.

[4] S. Zhang, H. Zhang *et al.*, "Joint trajectory and power optimization for UAV relay networks," *IEEE Commun. Lett.*, vol. 22, no. 1, pp. 161–164, Jan 2018.

[5] Q. Wu, J. Xu, and R. Zhang, "Capacity characterization of UAV-enabled two-user broadcast channel," *IEEE J. Sel. Areas Commun.*, vol. 36, no. 9, pp. 1955–1971, Sep. 2018.

[6] M. Shafi, A. F. Molisch *et al.*, "5G: A tutorial overview of standards, trials, challenges, deployment, and practice," *IEEE J. Sel. Areas Commun.*, vol. 35, no. 6, pp. 1201–1221, June 2017.

[7] G. Durisi, T. Koch, and P. Popovski, "Toward massive, ultrareliable, and low-latency wireless communication with short packets," *Proc. IEEE*, vol. 104, no. 9, pp. 1711–1726, Sept 2016.

[8] Y. Polyanskiy, H. V. Poor, and S. Verdu, "Channel coding rate in the finite blocklength regime," *IEEE Trans. Inf. Theory*, vol. 56, no. 5, pp. 2307–2359, May 2010.

[9] J. Li and Y. Han, "Optimal resource allocation for packet delay minimization in multi-layer UAV networks," *IEEE Commun. Lett.*, vol. 21, no. 3, pp. 580–583, March 2017.

[10] Q. Wu and R. Zhang, "Common throughput maximization in UAV-enabled OFDMA systems with delay consideration," *IEEE Trans. Commun.*, vol. 66, no. 12, pp. 6614–6627, Dec 2018.

[11] X. Lin, V. Yajnanarayana, S. D. Muruganathan, S. Gao, H. Asplund, H. Maattanen, M. Bergstrom, S. Euler, and Y. . E. Wang, "The sky is not the limit: Lte for unmanned aerial vehicles," *IEEE Commun. Mag.*, vol. 56, no. 4, pp. 204–210, April 2018.